Journal of Controlled Release 169 (2013) 211–219

Contents lists available at SciVerse ScienceDirect

Journal of Controlled Release

journal homepage: www.elsevier.com/locate/jconrel

NANOMEDICINE

Construction of block copolymers for the coordinated delivery of doxorubicin and magnetite nanocubes

Yong Wang, Nor Lizawati Ibrahim, Jiang Jiang, Shujun Gao, Nandanan Erathodiyil, Jackie Y. Ying *

Institute of Bioengineering and Nanotechnology, 31 Biopolis Way, The Nanos, Singapore 138669, Singapore

ARTICLE INFO

Article history:
Received 17 October 2012
Accepted 24 February 2013
Available online 15 March 2013

Keywords:
Co-delivery
Multifunctional nanoparticles
NMP
Doxorubicin
Iron oxide

ABSTRACT

Multifunctional nanoparticles combine drug and imaging agent together to assign both therapeutic and diagnostic functions. However, particle aggregation/dissociation and/or major differences in the bio-distribution and targeting capability of drugs and imaging probes are main obstacles for the efficient, coordinated delivery of multiple agents, unless the different agents can be tightly bound and well-protected during their circulation *in vivo*. In this paper, we report the coordinated *in vivo* delivery of anti-cancer drugs and imaging agents by chemically loading doxorubicin and magnetite nanocubes (MNs) in the core of polymeric nanoparticles. Living polymerization, nitroxide-mediated radical polymerization (NMP), was applied to construct the optimal polymers to co-deliver doxorubicin and MNs. The resulting diblock polymers consisted of one block with triethylene glycol brushes and another block with carboxylic acid groups to bind doxorubicin and Fe_3O_4 MNs. The optimal polymer has narrow polydispersity (PDI = 1.2) and high doxorubicin/MN loading (30 wt.%/28 wt.%). Core–shell particles were obtained with good stability and a suitable particle size of ~100 nm. The doxorubicin and MNs loaded in this polymeric system showed highly coordinated bio-distribution in the balb/C mice model. This system may have important impact on the design of effective and stable dual-agent co-delivery systems.

1. Introduction

Nanoparticles have received considerable attention as effective delivery vehicles for chemotherapeutic drugs due to their passive tumor-targeting properties, enhanced efficacy and reduced side effects. More recently, multifunctional nanoparticles have drawn a great deal of interest [1–18]. Some systems combine different imaging agents to provide for multimodal imaging [1a,2–4]. For example, a combination of quantum dots (QDs) and iron oxide magnetic nanoparticles would enable both fluorescence imaging and magnetic resonance imaging (MRI) [3]. Bigall et al. reviewed hybrid multifunctional colloidal nanomaterials that combine two or three imaging functions, e.g. fluorescence, magnetic and plasmonic [4]. Gorin et al. reported biocompatible microcapsules with magnetic and gold nanoparticles that are functionalized to be sensitive to laser irradiation [5]. Other systems allow for the co-delivery of drugs and imaging agents, providing for therapeutic and diagnostic effects simultaneously [2,6]. Such systems may deliver anti-cancer drugs (e.g. doxorubicin and paclitaxel) together with superparamagnetic iron oxide nanoparticles (SPIONs) [6–18]. Combining imaging agents with anti-cancer drugs enables the real-time monitoring of the drug distribution surrounding the target tissue, as well as the therapeutics' effect on disease progression [19]. Specifically, the nanosystems that combine anti-cancer drugs and SPIONs can be applied towards magnetically guided delivery [13,20], synergistic hyperthermia therapy and chemotherapy [21].

SPION (e.g., Feridex IV™ and Endorem™) have been widely used in MRI clinically for diagnostic applications; hence, they have been examined by many researchers as drug carrier systems [22]. The magnetic nanoparticles currently employed clinically are primarily dextran-coated iron oxides with good water dispersibility [23]. Several attempts have been made to use magnetic nanoparticles for drug delivery, while retaining their inherent magnetic and imaging properties. In most common approaches, the drug of interest is conjugated [8] or simply adsorbed [9] to dextran or other polymeric coatings, such as agarose, starch, polyethylene glycol (PEG) and block copolymers [8,9,20,23]. In such cases, the drug has relatively limited association with magnetic nanoparticles, and undergoes fairly rapid dissociation [20]. In addition, the drug's association with the particle surface can alter the physical and/or surface characteristics of the original magnetic nanoparticles (e.g. hydrodynamic size, charge, stability and magnetization) [24,25], which may influence the bio-distribution of magnetic nanoparticles [26], and thus, the imaging characteristics. For example, Li et al. reported agarose-stabilized magnetic colloidal nanocrystalline clusters with doxorubicin conjugated on the surface via pH-sensitive hydrazone. The surface property of the particles was changed due to the conjugation of doxorubicin, which may affect their stability *in vivo* [8]. In another approach, magnetic nanoparticles are dispersed in biodegradable polymers (e.g., polylactide and poly(lactide co-glycolide) that are typically used as nanocarriers for drug delivery

* Corresponding author. Tel.: +65 6824 7100; fax: +65 6478 9020.
E-mail address: jyying@ibn.a-star.edu.sg (J.Y. Ying).

0168-3659/$ – see front matter © 2013 Elsevier B.V. All rights reserved.
http://dx.doi.org/10.1016/j.jconrel.2013.02.024

applications [27]. However, this approach is usually limited due to water insolubility, and tends to form large microparticles with limited encapsulation of magnetic nanoparticles. Therefore, these carrier systems have an overall magnetization that may adversely impact both their drug targeting efficiency in response to an external magnetic field and their imaging properties [28–31].

Liposomes, emulsions and amphiphilic polymers have been applied to incorporate both the drug of interest and the imaging agents (including iron oxide) [16,17,32–34]. In these systems, the drugs and/or the imaging probes are incorporated physically, resulting in the rapid release of the drugs and/or imaging probes from the nanoparticles. Rapid release of the agents jeopardizes nanoparticle stability, and the different agents possess different targeting capabilities, resulting in major differences in the bio-distributions of drugs and imaging probes. Hence, it has been very challenging to coordinate the delivery of multiple agents and harness their synergistic effects, unless the different agents can be tightly bound during their circulation *in vivo*.

By utilizing a recently developed robust living polymerization method, NMP [35–37], we have synthesized a series of well-defined copolymers with narrow polydispersity to study the influence of polymer structure on the loading efficiency and stability of nanoparticles loaded with dual agents. The resulting polymers consisted of one block with triethylene glycol brushes to protect the particles from entrapment by reticuloendothelial system (RES), and other blocks with binding groups for chemical loading of doxorubicin and Fe_3O_4 MNs.

2. Materials and methods

2.1. Synthesis of block copolymers

Monomers illustrated in Scheme 1 have been synthesized (see Supporting Information (SI)) for use in the synthesis of diblock copolymers (Scheme 2). 4-Vinylbenzyl methoxy triethylene glycol ether (TEGSt) was employed in building the hydrophilic segment and protecting against the entrapment by RES. 4-Vinylbenzoic doxorubicin amide (DOXSt) was designed to introduce the building block with doxorubicin. 4-Vinylbenzyl cholesterol ether (CHOLSt) was synthesized to build the hydrophobic block that would not bind MNs and doxorubicin chemically. 4-Vinyl benzoic acid (VBA) was purchased and used as the monomer for building the block that bound MNs and conjugated doxorubicin randomly.

Five polymers with different structures were synthesized by NMP (Scheme 3). The initiator, TPPA, was freshly synthesized and characterized by ^{1}H nuclear magnetic resonance (NMR) spectroscopy (SI Scheme S1 and Figs. S1–S3). TEGSt, DOXSt and CHOLSt monomers were synthesized and characterized by general procedures (SI Figs. S4–S6).

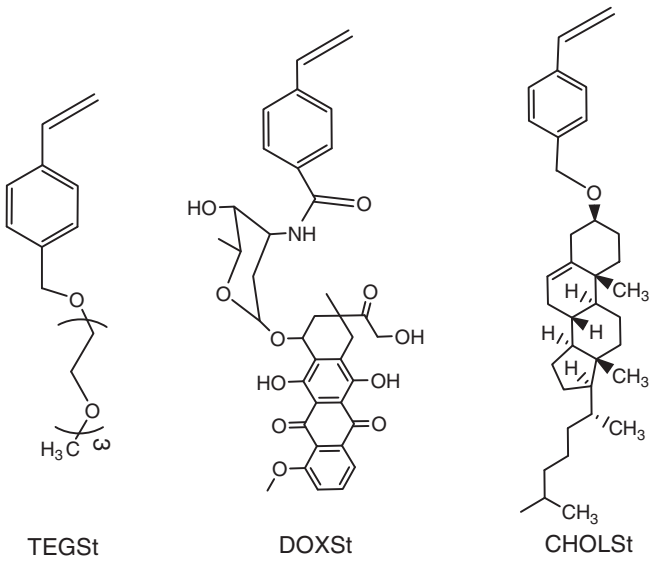

Scheme 1. Molecular structure of the monomers, TEGSt, DOXSt and CHOLSt.

2.1.1. Synthesis of polymer A

Diblock or triblock polymer A (poly(TEGSt-co-DOXSt-co-VBA)), polymer B (poly(TEGSt-co-VBA-co-DOXSt)), polymer C (poly(TEGSt-co-VBA)-DOX), polymer D (poly(TEGSt-co-VBA)) and polymer E (poly(TEGSt-co-CHOLSt)) were synthesized via a two- or three-step procedure using the living polymerization, NMP (Scheme 2). For synthesis of polymer A, TEGSt (1.23 g, 4 mmol) was added to a 10-ml ampule bottle with a stir bar, and was allowed to dissolve in 2 ml of anisole added with 2,2,5-trimethyl-3-(1-phenylethoxy)-4-phenyl-3-azahexane (TPPA) (13 mg, 0.043 mmol). The solution in the ampule bottle was degassed by freeze–pump–backfilling with nitrogen 6 times, and sealed with a blow torch. After warming to room temperature, the ampule was placed in a 130 °C oil bath, and stirred overnight. Next, the ampule was opened, and the solution was diluted with tetrahydrofuran (THF) and precipitated in hexane. The semi-solid product was redissolved in THF and reprecipitated in hexane to remove the unreacted monomer completely to obtain hydrophilic block poly(TEGSt), which will be used as macroinitiator for the reaction of another monomer. The semi-solid product was dried overnight in a vacuum oven (50 °C) with a yield of 1.0 g (81%). Next, the polymer obtained was dissolved in 5 ml of anisole again and added to a 10-ml ampule. 200 mg of DOXSt was added to the 10-ml ampule. After degassing with the freeze–pump–nitrogen gas refilling procedure six times (as described above) and sealing, the reaction was allowed to take place overnight at 130 °C. The product was diluted, and dialyzed against dimethyl sulfoxide (DMSO) for one day, followed by deionized water for another day (dialysis tubing's molecular weight cut-off (MWCO) = 3500 Da). The product was freeze-dried and redissolved in 6 ml of anisole before it was added to a 10-ml ampule to initiate the third monomer. 200 mg of 4-vinyl benzoic acid was added to the ampule. The ampule was degassed in the same manner as described earlier and sealed. It was allowed to react at 130 °C overnight. The solution was precipitated in ether twice, and dried in vacuum oven to obtain 0.84 g of product (SI Fig. S7).

2.1.2. Synthesis of polymer B

200 mg of 4-vinyl benzoic acid was added to a 10-ml ampule containing 1 g of poly(TEGSt) in anisole (2 ml) and a magnetic stir bar. The ampule was degassed by a freeze–pump–nitrogen gas refilling procedure six times, and sealed with a blow torch. After reaction at 130 °C overnight, the solution was precipitated twice in hexane. 1 g of dry product poly(TEGSt-co-VBA) was obtained. Next, 200 mg of DOXSt was added to a 10-ml ampule containing poly(TEGSt-co-VBA) dissolved in anisole (6 ml), degassed the same way as described above, and sealed. The system was allowed to react overnight at 130 °C. The solution was diluted by DMSO, and dialyzed against DMSO for one day and deionized water for another day (dialysis tubing's MWCO = 3500 Da). The product (0.90 g) was harvested by freeze drying (SI Fig. S8).

2.1.3. Synthesis of polymers C and D

Synthesis of polymer D was followed by polymer C. Briefly, 1 g of poly(TEGSt) dissolved in anisole was added to a 10-ml ampule bottle with a stir bar. Thereafter, 4-vinyl benzoic acid (300 mg, 2 mmol) was added. The solution in the ampule bottle was degassed by freeze–pump–refilling of nitrogen 6 times, and sealed with a blow torch. The ampule was warmed to room temperature, placed in a 130 °C bath, and stirred overnight. It was then unsealed, and the solution was diluted with THF and precipitated with ether twice to obtain 0.52 g of a light yellow solid product polymer D (SI Fig. S10). The molar percentages of the two blocks were estimated first by comparing the ratio of the ^{1}H NMR $(CH)_2$–CH_2– peak at δ 4.47 ($=\Delta_{TEGSt}/2$) (which was attributed to TEGSt) with the aromatic peak at δ 6–8